

134

Reprint Series  
27 July 1990, Volume 249, pp. 411-414

**SCIENCE**

## **Four-Dimensional Heteronuclear Triple-Resonance NMR Spectroscopy of Interleukin-1 $\beta$ in Solution**

LEWIS E. KAY, G. MARIUS CLORE, AD BAX, AND ANGELA M. GRONENBORN

Many of the uncertainties present in 2D NMR spectra can be resolved by spreading out the 2D spectra into a third dimension (6), and NMR techniques based on large heteronuclear couplings should permit applications to larger proteins (7). To this end a number of three-dimensional (3D) heteronuclear NMR experiments that rely on large resolved heteronuclear couplings have been developed (8–13) and have been shown to be highly efficient for spectral assignment of proteins labeled with  $^{15}\text{N}$  or  $^{13}\text{C}$  or both up to a molecular weight of about 20 kD (14). Despite this added resolution, ambiguities still remain in the interpretation of 3D heteronuclear NMR spectra of larger proteins, so that an additional increase in resolution afforded by raising the dimensionality still further is desirable. In this paper we report a four-dimensional (4D) NMR experiment and demonstrate its applicability to uniformly labeled  $^{15}\text{N}$ - $^{13}\text{C}$  interleukin-1 $\beta$  (IL-1 $\beta$ ), a 17.4-kD protein of 153 residues, that plays a central role in the immune and inflammatory responses (15).

All 2D NMR experiments comprise four distinct steps, namely, preparation, evolution, mixing, and detection (16). A 4D NMR experiment is easily conceived by combining three 2D NMR experiments, leaving out the detection period of the first, the preparation and detection periods of the second, and the preparation period of the third. The 4D experiment we have chosen to perform is one in which NOEs between NH protons and aliphatic protons are spread out by the chemical shifts of the directly bonded  $^{15}\text{N}$  and  $^{13}\text{C}$  atoms, respectively. The rationale behind this experiment lies in resolving extensive ambiguities still present in a 3D  $^{15}\text{N}$ -edited NOESY experiment (3D  $^1\text{H}$ - $^{15}\text{N}$  NOESY-HMQC) in which NOEs between NH protons and aliphatic protons are spread into the third dimension by the chemical shift of the directly bonded  $^{15}\text{N}$  atoms (8, 9). Although this 3D experiment effectively removes, in all but a very few cases, chemical shift degeneracy associated with the NH protons, it leaves the ambiguities associated with severe overlap of aliphatic resonances unaffected. Thus, even if a cross peak connecting an aliphatic and amide proton is well resolved in the 3D spectrum, it is frequently not possible, with the exception of cases involving the C $\alpha$ H resonances, to identify conclusively the aliphatic proton involved on the basis of its  $^1\text{H}$  chemical shift.

The progression and relation between  $^{15}\text{N}$ - $^{13}\text{C}$ -heteronuclear-edited 2D, 3D, and 4D NOESY experiments is illustrated schematically in Fig. 1. In the 2D spectrum, NOEs between NH protons ( $F_2$  dimension) and aliphatic protons ( $F_1$  dimension) are

## Four-Dimensional Heteronuclear Triple-Resonance NMR Spectroscopy of Interleukin-1 $\beta$ in Solution

LEWIS E. KAY, G. MARIUS CLORE, AD BAX, ANGELA M. GRONENBORN

A method is presented that dramatically improves the resolution of protein nuclear magnetic resonance (NMR) spectra by increasing their dimensionality to four. The power of this technique is demonstrated by the application of four-dimensional carbon-13–nitrogen-15 ( $^{13}\text{C}$ - $^{15}\text{N}$ )-edited nuclear Overhauser effect (NOE) spectroscopy to interleukin-1 $\beta$ , a protein of 153 residues. The NOEs between NH and aliphatic protons are first spread out into a third dimension by the  $^{15}\text{N}$  chemical shift of the amide  $^{15}\text{N}$  atom and subsequently into a fourth dimension by the  $^{13}\text{C}$  chemical shift of the directly bonded  $^{13}\text{C}$  atoms. By this means ambiguities in the assignment of NOEs between NH and aliphatic protons that are still present in the three-dimensional  $^{15}\text{N}$ -edited NOE spectrum due to extensive chemical shift overlap and degeneracy of aliphatic resonances are completely removed. Consequently, many more approximate interproton distance restraints can be obtained from the NOE data than was heretofore possible, thereby expanding the horizons of three-dimensional structure determination by NMR to larger proteins.

OVER THE LAST FEW YEARS IT HAS been shown that two-dimensional (2D) NMR spectroscopy (1) can be used to determine the solution structures of small proteins ( $\leq 100$  residues) at a resolution comparable to that attainable by x-ray crystallography (2–4). The initial stage in an NMR structure determination involves spectral assignment by means of experiments that demonstrate through-bond and through-space correlations (5). The principal source of geometric information resides in short ( $< 5$  Å) approximate interproton

distance restraints derived from NOE experiments, and the accuracy and precision of an NMR structure determination depends critically on the number of restraints that can be extracted from the data (3, 4). The application of 2D NMR methods to larger proteins has been impeded by two factors. First, the increase in the number of resonances leads to severe chemical shift overlap and degeneracy, rendering the assignment of through-bond interactions or through-space interactions or both increasingly difficult. Second, the increase in molecular weight results in larger linewidths so that the sensitivity of through-bond correlation experiments based on small ( $< 12$  Hz) homonuclear couplings is much reduced.

Laboratory of Chemical Physics, National Institute of Diabetes and Digestive and Kidney Diseases, National Institutes of Health, Bethesda, MD 20892.

observed in a single plane. In the 3D spectrum, these NOEs are spread within a 3D cube over a series of  $F_3(\text{NH})$ - $F_1(^1\text{H})$  slices according to the chemical shift of the directly bonded  $^{15}\text{N}$  atoms in the  $F_2$  dimension. In the 4D experiment, each slice at a particular  $^{15}\text{N}$  frequency of the 3D spectrum constitutes a cube within the 4D spectrum in which each cube is subdivided into a further series of slices based on the  $^{13}\text{C}$  chemical shift of the  $^{13}\text{C}$  atoms directly bonded to the aliphatic protons indicated in  $F_1$ .

The pulse scheme of the new 4D experiment is shown in Fig. 2. It combines three separate 2D experiments, namely  $^1\text{H}$ - $^{13}\text{C}$  HMQC,  $^1\text{H}$ - $^1\text{H}$  NOESY, and  $^1\text{H}$ - $^{15}\text{N}$  HMQC sequences. Transfer of magnetization between protons and the directly bonded  $^{15}\text{N}$  or  $^{13}\text{C}$  heteronucleus is achieved by means of multiple quantum coherence (17),

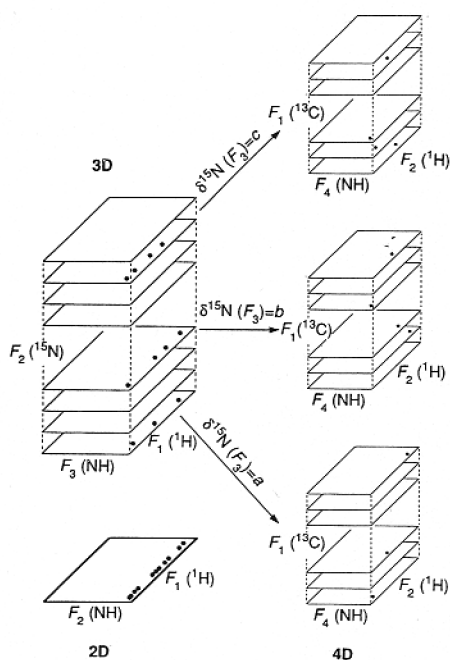
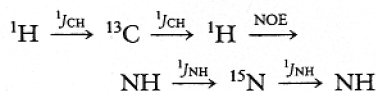


**Fig. 1.** Schematic illustration of the progression and relation between heteronuclear edited 2D, 3D, and 4D NOESY spectra. The closed circles represent NOE cross peaks between NH and aliphatic protons. In the 2D spectrum, cross peaks from 11 aliphatic protons to 3 NH protons at a single NH chemical shift are indicated. In the 3D spectrum, these peaks are spread into a third dimension according to the chemical shift of the directly bonded  $^{15}\text{N}$  atoms. In the illustration the peaks are now located in three distinct planes corresponding to three different  $^{15}\text{N}$  chemical shifts, thereby removing the overlap arising from NH chemical shift degeneracy and indicating that the NOEs involve three separate NH protons. Although the NH protons are resolved in the 3D spectrum, the identity of the aliphatic protons can still only be established by their  $^1\text{H}$  chemical shifts. In the 4D spectrum, each plane of the 3D spectrum constitutes a cube composed of a series of slices at different  $^{13}\text{C}$  chemical shifts. The identity of the originating aliphatic protons can now be established unambiguously as they are characterized by both  $^1\text{H}$  and  $^{13}\text{C}$  chemical shifts.

whereas transfer of magnetization between protons occurs by through-space NOE effects. The transfer of magnetization from the aliphatic protons to the NH protons thus follows the pathway:



The chemical shifts of  $^{13}\text{C}$ ,  $^1\text{H}$ , and  $^{15}\text{N}$  evolve during the variable time periods  $t_1$ ,  $t_2$ , and  $t_3$ , which are incremented independently, and the NH signal is acquired during the acquisition period  $t_4$ . A 4D Fourier transformation of the resulting data matrix with respect to  $t_1$ ,  $t_2$ ,  $t_3$ , and  $t_4$  yields a 4D spectrum in which every NOE interaction between an NH proton and an aliphatic proton is determined by four frequency coordinates, the chemical shift values of the two protons involved in the  $F_2$  and  $F_4$  dimensions and the chemical shifts of the  $^{13}\text{C}$  and  $^{15}\text{N}$  nuclei attached to these two protons in the  $F_1$  and  $F_3$  dimensions, respectively. Signal not originating from an aliphatic proton or terminating on an amide proton is efficiently canceled by appropriate phase cycling of the  $^{13}\text{C}$  and  $^{15}\text{N}$  pulses, as indicated in the caption to Fig. 2. Three key aspects of practical importance should be noted. The first is that the number of peaks

in this 4D spectrum is the same as that present in the corresponding  $^{15}\text{N}$ - $^{13}\text{C}$ -edited 3D and 2D spectra. Thus, the extension to four dimensions affords an increase in resolution without a concomitant increase in complexity. Second, the through-bond transfer steps are highly efficient as they involve couplings (90 to 130 Hz) that are much larger than the linewidths. Consequently the sensitivity of the 4D experiment is high. Third, extensive folding is used to maximize resolution in the  $^{13}\text{C}(F_1)$  dimension (10, 18). As a result, each  $^{13}\text{C}$  coordinate corresponds to a series of  $^{13}\text{C}$  chemical shifts that, in the present case, are separated by intervals of 20.71 ppm. This process does not complicate the interpretation of the 4D spectrum in any way since all  $^{13}\text{C}$  resonances of IL-1 $\beta$  have been assigned (14) and the appropriate  $^{13}\text{C}$  chemical shift is readily determined from the  $^1\text{H}$  chemical shift of the aliphatic proton from which the magnetization originates (10, 12).

Selected  $F_4(\text{NH})$ - $F_2(^1\text{H})$  slices of the 4D  $^{13}\text{C}$ - $^{15}\text{N}$ -edited NOESY experiment of 1.7 mM  $^{13}\text{C}$ - $^{15}\text{N}$ -labeled IL-1 $\beta$  at two  $^{15}\text{N}(F_3)$  and several  $^{13}\text{C}(F_1)$  frequencies are shown in Fig. 3, together with the corresponding  $F_3(\text{NH})$ - $F_1(^1\text{H})$  slices of the 3D  $^{13}\text{C}$ - $^{15}\text{N}$ -edited  $^1\text{H}$ - $^{15}\text{N}$  NOESY-HMQC spectrum at the same  $^{15}\text{N}(F_2)$  chemical shifts. The 4D

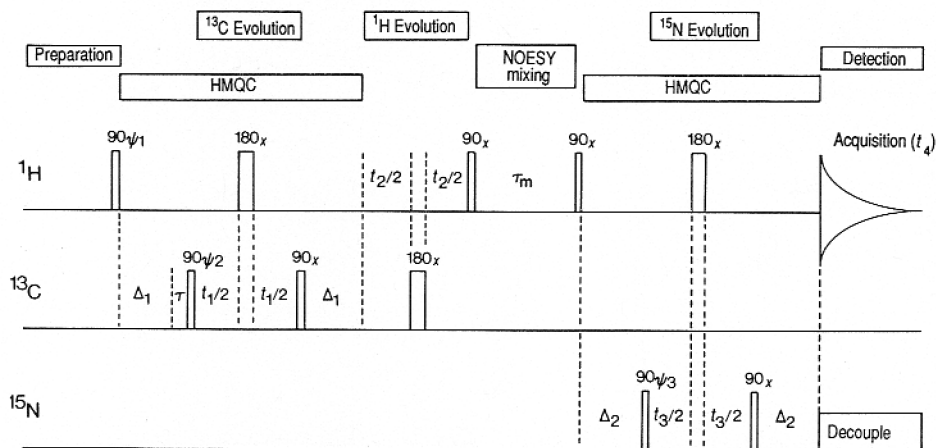


**Fig. 2.** Pulse sequence of the  $^{13}\text{C}$ - $^{15}\text{N}$ -edited NOESY 4D experiment. Water suppression is performed during both the relaxation delay and NOE mixing period with an off-resonance DANTE scheme (18). In order to minimize relaxation losses, the delays  $\Delta_1$  and  $\Delta_2$ , which allow for efficient creation of heteronuclear multiple quantum coherence, are set to 3.0 and 4.5 ms, slightly less than  $1/(2J_{\text{HC}})$  and  $1/(2J_{\text{HN}})$ , respectively. The NOE mixing time  $\tau_m$  was set to 96 ms. The delay  $\tau$  immediately prior to application of the first  $^{13}\text{C}$   $90^\circ$  pulse is included to compensate for the  $^{13}\text{C}$   $180^\circ$  pulse so that no first-order phase correction is necessary in  $F_2$ . The  $^1\text{H}$ ,  $^{13}\text{C}$ , and  $^{15}\text{N}$  carriers were positioned at 8.1, 43.0, and 121.0 ppm, respectively, and  $^{13}\text{C}$  and  $^{15}\text{N}$  radio frequency (rf) power levels of 16.7 and 1.25 kHz were used for all pulses. WALTZ decoupling (20) was performed during acquisition with a 1.25-kHz rf field. The phase cycling used was:  $\psi_1 = 4(x)$ ,  $\psi_2 = 2(x, -x)$ ,  $\psi_3 = 2(x), 2(-x)$ , and acquisition =  $x, -x, -x, x$ . Quadrature in the  $t_1$ ,  $t_2$ , and  $t_3$  dimensions was achieved by changing the phases of  $\psi_1$ ,  $\psi_2$ , and  $\psi_3$  by  $90^\circ$  in an independent manner with the States-TPPI method (21). The spectrum was recorded with sequential quadrature detection during the detection period  $t_4$ . The experiment was recorded on a Bruker AM-600 spectrometer equipped with a triple-resonance probe optimized for  $^1\text{H}$  detection. The acquired 4D data matrix comprised 16 complex ( $t_1$ ) by 64 complex ( $t_2$ ) by 16 complex ( $t_3$ ) by 512 real ( $t_4$ ) data points. The delays and pulse widths in the sequence were chosen such that the phase of the folded peaks in  $F_1$  is the same as those that are not folded (18). The spectral widths used in  $F_1$ ,  $F_2$ ,  $F_3$ , and  $F_4$  are 20.71, 8.3, 26.0, and 6.94 ppm, respectively, with corresponding acquisition times of 5.0, 12.6, 9.8, and 61.4 ms in  $t_1$ ,  $t_2$ ,  $t_3$ , and  $t_4$ , respectively.

experiment was recorded in only 6 days, whereas the 3D data set was obtained in 1 day. The two slices of the 3D spectrum at  $\delta^{15}\text{N} = 118.1$  and  $119.8$  ppm represent typical planes in the 3D spectrum. The spectral simplification in the 4D slices relative to the 3D ones is obvious. Examination of the two 3D slices reveals a large number of NOEs between NH protons and aliphatic protons resonating between 5.5 and 0 ppm. Those involving intraresidue NH-C $\alpha$ H NOEs can be readily identified by comparison with a 3D  $^1\text{H}$ - $^{15}\text{N}$  HOHAHA-HMQC spectrum (9) in which correlations between NH and aliphatic protons are established through intraresidue scalar  $^3J_{\text{HN}\alpha}$  couplings. Providing the amino acid sequence is known and some spin systems have been identified, it is also usually possible to assign the sequential C $\alpha\text{H}(i)$ -NH( $i+1$ ) NOEs from the 3D spectrum with confidence. The remaining NOEs, and in particular those involving long-range interactions between residues far apart in the sequence, are very difficult and often impossible to interpret in the 3D spectrum because of extreme crowding and overlap of aliphatic  $^1\text{H}$  resonances. For example, between 1.2 and 0.8 ppm alone, there are 57 separate  $^1\text{H}$  resonances (14). Thus, although the destination NH proton can be uniquely defined in the 3D spectrum, there remains a large choice for the identity of the originating aliphatic proton. By spreading out the NOEs between NH and aliphatic protons on the basis of both  $^{15}\text{N}$  and  $^{13}\text{C}$  chemical shifts in the 4D spectrum, this problem is completely removed, and the specific identification of NOE interactions is reduced to matching all four chemical shifts with a database of complete  $^1\text{H}$ ,  $^{13}\text{C}$ , and  $^{15}\text{N}$  assignments previously obtained by analysis of a series of 3D heteronuclear double- and triple-resonance spectra (14). As an example, consider the NOEs between an aliphatic  $^1\text{H}$  resonance at 0.89 ppm and the NH protons of Ser<sup>21</sup>, Leu<sup>27</sup>, Gln<sup>39</sup>, and Val<sup>58</sup>. The two NOEs involving Leu<sup>21</sup>(NH) and Leu<sup>27</sup>(NH) are seen in the slice at  $\delta^{13}\text{C}$  values of 65.88, 45.17, and 24.46 ppm, whereas those involving Gln<sup>39</sup>(NH) and Val<sup>58</sup>(NH) are observed in the slice at  $\delta^{13}\text{C}$  values of 63.25, 42.54, and 21.83 ppm. From the  $^1\text{H}$  and  $^{13}\text{C}$  assignments already in hand, we conclude that the NOEs to Leu<sup>21</sup>(NH) and Leu<sup>27</sup>(NH) involve one of the methyl groups of Leu<sup>26</sup>. The NOEs to Gln<sup>39</sup>(NH) and Val<sup>58</sup>(NH) could involve a methyl group of either Val<sup>19</sup> or Val<sup>100</sup>. However, the NOE to Val<sup>58</sup>(NH) is maximal in this slice, whereas that to Gln<sup>39</sup>(NH) is maximal in the adjacent slice downfield in  $^{13}\text{C}$  chemical shift, indicating that they arise from methyl groups with different  $^{13}\text{C}$  chemical

shifts. This enables us to deduce that the NOE to Val<sup>58</sup>(NH) originates from Val<sup>100</sup>(C $\gamma^b\text{H}_3$ ), whereas that to Gln<sup>39</sup>(NH) is from Val<sup>19</sup>(C $\gamma^a\text{H}_3$ ).

In conclusion, we have demonstrated that  $^{13}\text{C}$ - $^{15}\text{N}$ -edited 4D NOESY spectroscopy is a powerful and conceptually simple approach for completely removing ambiguities

associated with valuable through-space connectivities between aliphatic and NH protons. Further, the spectra can be obtained with high sensitivity on  $\sim 1$  to 2 mM  $^{15}\text{N}$ - $^{13}\text{C}$ -labeled protein samples in a reasonable amount of measuring time. There are two fundamentally different approaches for increasing the resolution in protein NMR

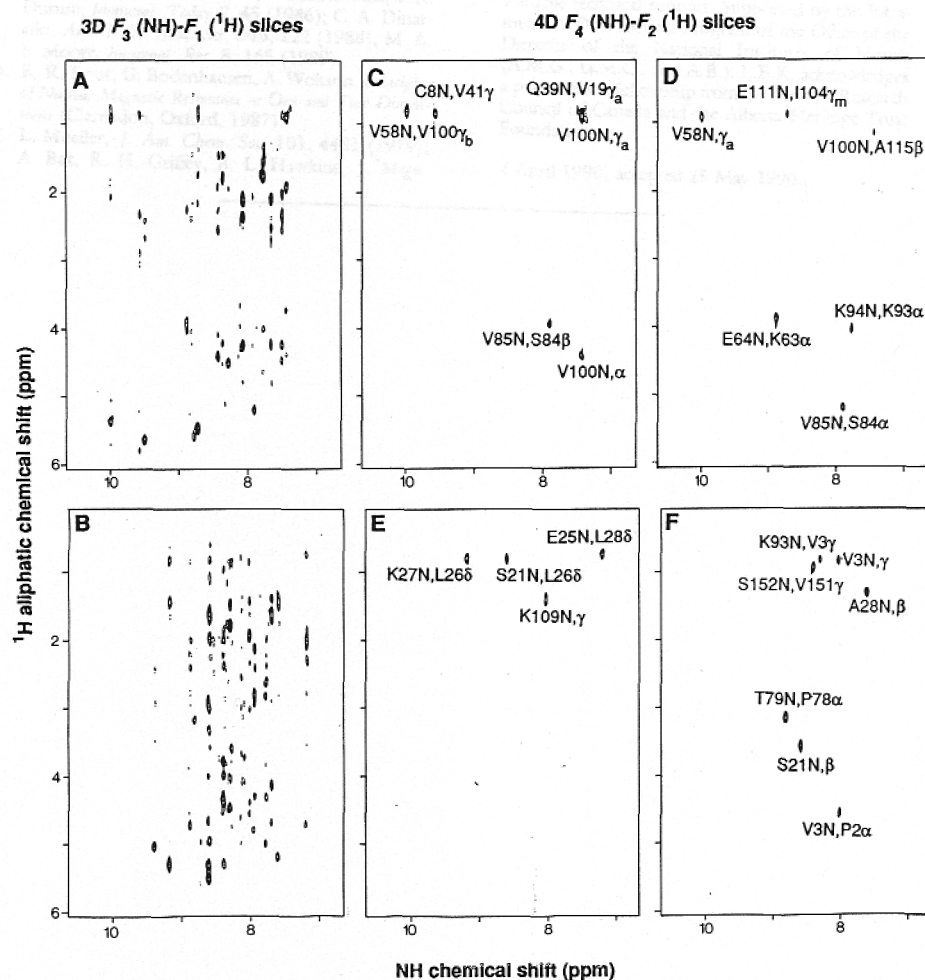


**Fig. 3.** Representative  $F_4(\text{NH})$ - $F_2(^1\text{H})$  planes of the 4D  $^{15}\text{N}$ - $^{13}\text{C}$ -edited NOESY spectrum together with the  $F_3(\text{NH})$ - $F_1(^1\text{H})$  slices of the 3D  $^{15}\text{N}$ - $^{13}\text{C}$ -edited NOESY spectrum at the corresponding  $^{15}\text{N}$  frequencies. Peak assignments were derived on the basis of the complete  $^1\text{H}$ ,  $^{15}\text{N}$ , and  $^{13}\text{C}$  assignments obtained from the analysis of a variety of 3D heteronuclear double and triple-resonance experiments (14). The 3D and 4D data sets were processed with an approach described previously (18). For the 3D slices, the  $^{15}\text{N}(F_2)$  values (parts per million) are 118.1 for (A) and 119.8 for (B). For the 4D slices, the  $^{15}\text{N}(F_3)$  values (ppm) are 118.1 for (C) and (D) and 119.8 for (E) and (F), and the  $^{13}\text{C}(F_1)$  values (ppm) are 63.25, 42.54, and 21.83 for (C), 58.65, 37.94, and 17.23 for (D), 65.88, 45.17, and 24.46 for (E), and 62.59, 41.88, and 21.17 for (F). A time-domain convolution routine (22) was used for both 3D and 4D data sets to remove the baseline distortion arising from the residual water resonance. In the case of the 3D  $^{15}\text{N}$ - $^{13}\text{C}$ -filtered NOESY data set, a doubly phase shifted sine bell window extending from  $60^\circ$  on the left to  $165^\circ$  on the right-hand side was used prior to transformation in  $F_2$ . One zero filling of the data was used in  $F_2$  with double zero filling in the other two dimensions. A simple in-house routine was used for the  $F_2$  Fourier transform whereas commercially available software (NMRI, Syracuse, New York) was used to process the  $F_1$ - $F_3$  planes. Processing of the 4D data set was done in several stages. Initially the data were processed in  $F_3$  with in-house written routines. A doubly shifted sine bell extending from  $60^\circ$  to  $165^\circ$  was used as well as a single zero filling prior to Fourier transformation. After the  $F_3$  transformation, a set of 32 3D data matrices filtered by the  $^{15}\text{N}$  chemical shift was generated. Processing of the  $^{13}\text{C}$  dimension ( $F_1$ ) was accomplished next. A doubly shifted sine bell extending from  $65^\circ$  to  $170^\circ$  was used followed by double zero filling and Fourier transformation with software developed in-house. Finally, individual  $F_2$ - $F_4$  planes were processed with commercially available software. The  $t_3$  processing and subsequent transformation required approximately 12 hours on a Sun Sparc workstation, with an additional 1 to 2 hours required for the processing of each of the resultant 32 3D data sets. The final digital resolution in each of the four dimensions was 48.8, 19.5, 49.4, and 4.1 Hz per point in  $F_1$ ,  $F_2$ ,  $F_3$ , and  $F_4$ , respectively.